Impact of room airflow interaction on metabolic CO_2 exposure

Athanasia Keli[1,*], *Arsen K.* Melikov[1], *Mariya P.* Bivolarova[1], and *Panu* Mustakallio[2]

[1]International Centre for Indoor Environment and Energy, Department of Civil Engineering, Technical University of Denmark, 2800 Kgs. Lyngby, Denmark
[2]Halton Oy, Haltonintie 1-3, 47400 Kausala, Finland

Abstract. CFD simulations were performed to investigate occupants' exposure to metabolic CO_2 in a room with mechanical ventilation. A meeting room occupied by six adult people performing sedentary activity was simulated. Five of the six occupants were simulated to exhale air with realistic CO_2 content, while one occupant was inhaling, i.e. the exposed occupant. Both exhalation and inhalation were simulated with constant flow rates. Two air distribution patterns were considered, mixing and displacement air distribution, each was combined with chilled ceiling, as summer conditions were simulated. For both air distribution patterns, the influence of solar gain of 200 W, which was simulated as heated vertical surface (window), and the distance between the occupants facing each other were studied. The simulation results revealed the importance of buoyancy flows generated by heated vertical surfaces for the pollution distribution. It was found out that compared to the case without solar heat gain, the presence of solar gain increased the inhaled CO_2 level by 26.9 % in the case of displacement ventilation, while it reduced the exposure by 4.5 % when the outdoor air was distributed by mixing ventilation. The distance between the occupants facing each other did not affect considerably the exposure.

1 Introduction

One of the environmental factors highly affecting the well-being and comfort of humans is the indoor air [1-3]. In order to assure clean air for breathing with no health hazards for occupants and thus to improve their comfort and performance, it is highly important to remove or dilute the pollutants present indoors. Therefore, the quality of air inhaled by occupants strongly depends on the ventilation that supplies clean outdoor air to spaces.

The most common type of mechanical ventilation used at present is the Total Volume Ventilation (TVV), i.e. entire room volume is ventilated. Two total volume air distribution patterns are mainly used today, namely mixing air distribution (mixing ventilation, MV) and displacement air distribution (displacement ventilation, DV). A simple parameter used to calculate and regulate the airflow rates in order to limit the level of pollution in rooms is the indoor CO_2 concentration [4].

So far, when using MV, it is assumed that the occupied zone is characterized by uniform pollution distribution, and the indoor CO_2 concentration is monitored by sensors installed either at the exhaust terminals or on a wall. However, numerous studies have shown that the concentration measurements at a reference location in a ventilated room may not be representative for the pollutants' concentration in the inhaled air [5-8].

Factors causing this non-uniform distribution of pollutants in the vicinity of an occupant is the free (natural) convection flow around a human body, the occupant's movement, the breathing, the pollution source location, the overall room airflow pattern, etc. [6, 9, 10]. The overall room airflow pattern is influenced by the strength of the heat loads, the distribution of the heat loads, the room geometry and the layout of furniture, as well as by the air distribution principle itself [11-14].

The purpose of the present study was to investigate by performing CFD (Computational Fluid Dynamic) simulations the influence of the heat gain from a vertical surface, assumed as solar gain from window, and the distance between the occupants facing each other in a meeting room on the airflow characteristics and exposure to metabolic CO_2. The importance of these two factors was studied with MV and DV.

2 Computational models

In this study, a commercial CFD program, Flovent 12.0, was used as a computational tool.

2.1 Geometry and boundary conditions

A meeting room with dimensions of 4.2 x 4.1 x 2.9 m^3 occupied by six adult occupants performing sedentary activity was modelled. The three cases presented in Table 1 were simulated two times, one with MV and the other with DV. Each air distribution pattern was combined with chilled ceiling. The target air

* Corresponding author: keliathanasia@outlook.com.gr

temperature, in the occupied zone in the case of MV and at 1.1 m above floor in the case of DV, was 26ºC to satisfy the requirements for buildings Category II indoor climate for summer conditions imposed by DS/EN 15251 [15].

Table 1. Simulated cases

Case 1: Reference case	Exposed occupant: No. 6 (Fig. 2 and Fig. 3). Distance between the occupants facing each other: 1.4 m. No solar gain.
Case 2: Solar gain	Exposed occupant: No. 6 (Fig. 2 and Fig. 3). Distance between the occupants facing each other: 1.4 m. Solar gain of 200 W.
Case 3: Smaller distance	Exposed occupant: No. 6 (Fig. 2 and Fig. 3). Distance between the occupants facing each other: 1 m. No solar gain.

In each case, five of the six occupants were simulated to exhale continuously, and one, the exposed occupant, was simulated to inhale continuously. The outdoor airflow rate was set to 44 L/s in order to keep the indoor CO_2 concentration equal to 1000 ppm, based on the requirements imposed by BR18 [4]. The required ventilation rate was calculated by using the mass balance equation for CO_2 concentration (Eq.1), assuming complete mixing of room air and steady-state conditions. The CO_2 concentration in the supplied outdoor air was set at 400 ppm. The calculations were based on CO_2 rate generated by the five exhaling occupants. An adult person performing sedentary activity (1 to 1.2 MET) generates on average CO_2 of 19 L/h [15], i.e. total CO_2 generation rate in the room equal to 5 x 19 L/h.

$$q = G_{CO2} / (C_{h,i} - C_{h,o}) \times 10^6 \quad (1)$$

Where, $C_{h,i}$ is the maximum allowed volume fraction of CO_2 in the indoor air, ppm; $C_{h,o}$ is the CO_2 volume fraction in the supplied outdoor air, ppm; G_{CO2} is the CO_2 generation rate in the room at room conditions, L/s; q is the required ventilation rate, L/s.

The internal heat loads considered in the CFD simulations are defined in Table 2. Only sensible heat was simulated.

Table 2. Internal heat gains

	Number x Heat load (W)	Total heat load (W)
Luminaries	4 x 40	160
Occupants' Body	6 x 74	444
Exhalation	5 x 0.84	4.2
Total		608.2

The simulation with the heat load defined in Table 2 was used as a reference case, respectively in the case of MV and DV. The solar gain was simulated by adding additional heat load of 200 W, i.e. the total heat gain was 808.2 W (both in the case of MV and DV).

Note that although as pollution sources were considered the five exhaling occupants, in the case of heat load, the heat emitted by all six occupants was taken into account.

The occupants were simulated with three cuboids that corresponded respectively to the upper part of the body (head and torso), thighs and legs (Fig. 1). The total surface area of the occupant's body in contact with the ambient air was 1.66 m^2. The sensible heat load of 74 W from each occupant's body was divided into convection and radiation, each part accounting respectively for 40 % and 60 % of the total sensible heat load [16]. The convective part of the sensible heat was distributed to the three cuboids, and it was simulated as fixed heat flow (Table 3).

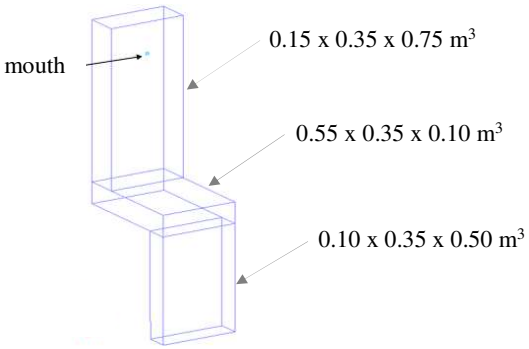

Fig. 1. Geometry of occupant's body

Table 3. Fixed heat flows attached to the cuboids comprising the human body

Cuboids	Fixed heat flow
Head and torso	20.72 W (70% of the convective heat)
Thighs	4.44 W (15% of the convective heat)
Legs	4.44 W (15% of the convective heat)

For the five occupants simulating continuous exhalation, exhalation through the mouth was assumed in all cases. The size of the mouth was 1.3 cm^2 (1.3 cm x 1 cm), as suggested in the literature for the mouth opening [17, 18]. The exhalation was simulated as fixed flow with inflow boundary conditions. The exhalation volume flow rate was set to be constant at 6 L/min, as suggested in the literature when the focus is on the expired air dispersion [19]. This value corresponded to the same pulmonary ventilation rate of an adult person performing sedentary activity [20]. The initial peak speed of the exhalation jet was manually calculated equal to 0.8 m/s. The flow direction of exhalation was set to be horizontal. The temperature of exhaled air was set to 34ºC. Taking into account the CO_2 generation rate of an adult person performing sedentary activity, the exhalation flow rate and the temperature of exhaled air, the CO_2 concentration in the exhaled air was calculated to be 52778 ppm (0.0806 kg/kg). The continuous inhalation of the last (sixth) occupant was simulated as a fixed flow with outflow boundary conditions and constant volume flow rate of 6 L/min. Inhalation through the mouth was assumed in all simulated cases. The size of the mouth of the occupant inhaling was the same as that of the occupants exhaling.

In the case of MV, the air was supplied by two ceiling diffusers (Fig. 2). Each diffuser supplied 22 L/s.

The diffuser was simulated as a cuboid with dimensions of 0.06 x 0.472 x 0.02 m^3 (Fig. 2). Fixed flows with inlet boundary conditions were attached to the two faces discharging the air. On each face, five fixed flows with horizontal direction were attached (Fig. 2). The ventilation air was supplied with a temperature of 18°C. The CO_2 concentration in the supplied air was set to 0.0006117 kg/kg, corresponding to 400 ppm at supplied air temperature of 18°C.

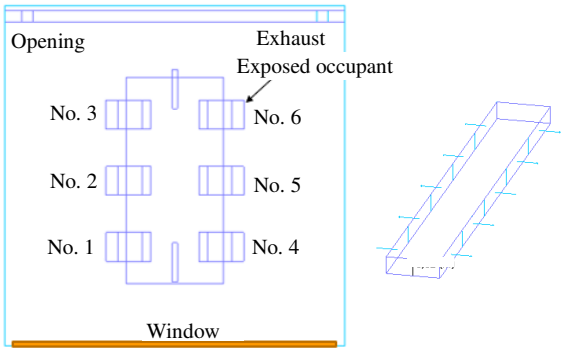

Fig. 2. Left: MV room; Right: MV diffuser

In the case of DV, the outdoor air was distributed by one rectangular perforated diffuser placed below the window (Fig. 3). The diffuser was simulated as a cuboid with dimensions of 0.54 x 0.07 x 0.32 m^3 (Fig. 3). Five fixed flows with inlet boundary conditions were attached to the face discharging the air (Fig. 3). The velocity vector of each fixed flow was modified in the x-z plane to simulate the semi-circular air discharge. The free area ratio of each fixed flow was 60 %. The ventilation air was supplied with a temperature of 20°C. The CO_2 concentration in the supplied air was set to 0.0006111 kg/kg, corresponding to 400 ppm at supplied air temperature of 20°C.

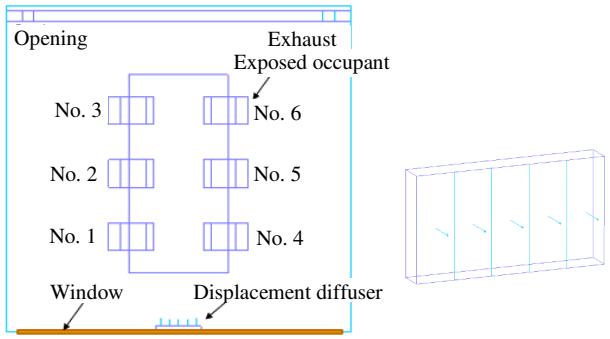

Fig. 3. Left: DV room; Right: DV diffuser

With the used airflow rate and temperature of supplied air, either with MV or DV, it was possible to remove only part of the total sensible heat load. To remove the surplus heat and maintain the air temperature, in the occupied zone in the case of MV and at 1.1 m above floor in the case of DV, at 26°C, a chilled ceiling was simulated. The chilled ceiling was simulated as a collapsed cuboid with size of 4.2 x 4.1 m^2. The required cooling capacity of the chilled ceiling, as well as the heat exchange through ventilation are presented in Table 4. To simulate the cooling power, fixed temperature was attached to the cooling ceiling object. The required ceiling temperature was calculated by using Eq. 2.

$$q_c = 8.92 \times (T_i - T_{s,m})^{1.1} \quad (2)$$

Where, q_c is the required cooling capacity of the chilled ceiling in W/m^2; T_i is the target indoor temperature in °C; $T_{s,m}$ is the surface temperature of the chilled ceiling in °C.

Table 4. Required cooling capacity and surface temperature of the chilled ceiling, and heat exchange through ventilation

	MV	DV
Heat outflow through ventilation	391.6 W	338.2 W
q_c, no solar gain	12.6 W/m^2	15.7 W/m^2
q_c, solar gain of 200 W	24.2 W/m^2	27.3 W/m^2
$T_{s,m}$, no solar gain	24.64°C	24.34°C
$T_{s,m}$, solar gain of 200 W	23.53°C	23.25°C

Without considering the solar gain, the walls, window and floor had the same surface temperature attached in order to simulate the radiant part of the sensible heat of the occupants' body and lighting, corresponding to 426.4 W. The heat load from the lighting units was assumed only as radiant heat load. To find the correct value of the attached temperature, an iterative process was followed in order to achieve heat balance in the room. In the simulated case in which solar gain of 200 W was considered (Case 2, Table 1), fixed temperature of 30°C was attached to the surface of the window, and the fixed temperature of the walls and floor was modified accordingly to achieve heat balance. The required temperature of the surface of the window to simulate the solar gain of 200 W was calculated by using Eq. 3. The window was placed 0.75 m above floor (Fig. 4). The window area was 6.3 m^2.

$$T_{window} = (q_s / 8) + T_i \quad (3)$$

Where, q_s is the heat flux in W/m^2 (solar gain of 200 W divided by the area of the window); T_i is the indoor air temperature, 26°C.

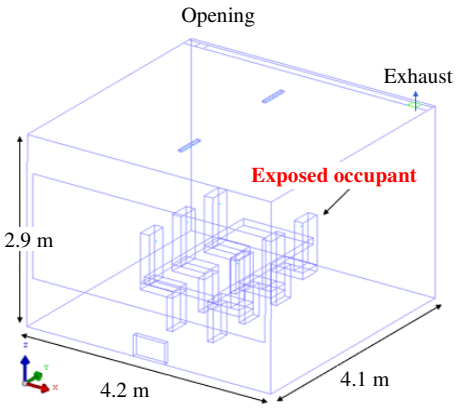

Fig. 4. Modelled domain

The two ceiling exhausts were modelled as rectangular surfaces with a size of 0.14 x 0.14 m^2 (Fig.

4). One was simulated as fixed flow with outflow boundary conditions. To achieve air pressure balance in the room, as five occupants were exhaling and only one was inhaling, the total outflow volume rate was defined at 44.4 L/s, corresponding to the sum of the total inflow volume rate through ventilation and the volume flow rate exhaled by four occupants. The other exhaust was simulated as an opening corresponding to a pressure outlet with defined pressure of 0 Pa. This distribution of the exhaust air helped to obtain convergence of the CFD simulations.

A table was modelled in the center of the room, at a height of 0.75 m above floor (Fig. 4). The distance of the occupants' "torso" from the table was always 0.1 m. In Cases 1 and 2 (Table 1), the dimensions of the table were 1.2 x 2.5 x 0.1 m^3 and the distance between the occupants facing each other seated on the long side of the table was 1.4 m. In Case 3 (Table 1) the distance between the occupants seated on the long side of the table was decreased to 1 m. In that case, the width of the table decreased to 0.8 m as well. In all cases the distance between the occupants sitting next to each other was 0.45 m.

2.2 Equations, grid and convergence

The model was three-dimensional, time-independent and non-isothermal with the participation of two species, air and CO_2. The numerical model solved the continuity, momentum, energy, turbulence conservation and chemical species equations. The airflow was modelled by using the LVEL k-ε model. The radiant part of the heat exchange was simulated by attaching the required temperature to the surfaces of the envelope in order to obtain heat balance without enabling the radiation model in the CFD simulations.

The mesh consists of a main region with grid patches in the edges, and regions of localized grid around occupants, diffuser(s) and close to the domain enclosure. The maximum size of the cells of the system grid was set to 5 cm. The size of the cells in regions with fine grid varied accordingly to complexity of the flow. The total number of the cells varied between the simulated cases, but in all cases it was higher than 623000 cells. In all cases, the maximum aspect ratio of the cells was below 5.

The solution was considered to be converged by taking into account the following criteria: Residual values of the Navier-Stokes equations, changes of monitored variables, and heat and mass balances. The monitoring variables were the air pressure, air velocities, air temperature, CO_2 concentration, air density, turbulence and viscocity. The criteria for the acceptance of the residual values was set as a drop below 10 (3 orders of magnitude). The variables were monitored at several points.

3 Results and discussion

Fig. 5 and Fig. 6 present the CO_2 concentration monitored at the mouth of the exposed occupant (Occupant No. 6) and above the occupants at a vertical distance from the head of 10 cm, in the three considered cases (Table 1) when using DV and MV, respectively. For both air distribution patterns, the exposure and CO_2 distribution were affected mostly by the simulation of the solar gain. These results document the importance of the airflow interaction in a room, and in particular, the importance of buoyancy flows generated by heated vertical surfaces (window) for the pollution distribution. The distance between the occupants facing each other did not affect considerably the exposure.

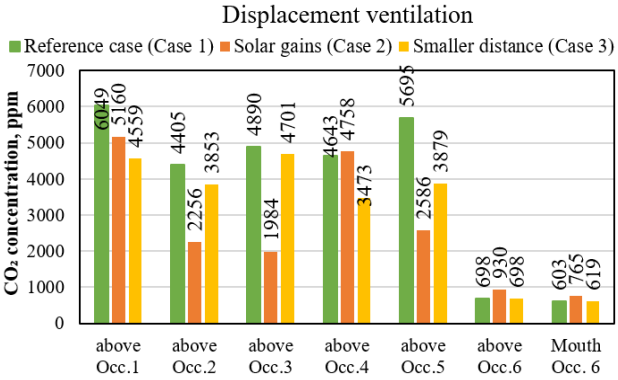

Fig. 5. CO_2 levels monitored at the mouth of the exposed occupant (Occ. No. 6) and above the occupants' heads in the different simulated cases that the air supply was done by DV

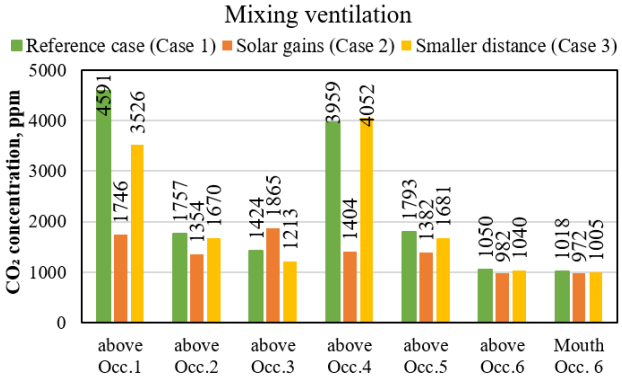

Fig. 6. CO_2 levels monitored at the mouth of the exposed occupant (Occ. No. 6) and above the occupants' heads in the different simulated cases that the air supply was done by MV

Using MV, the CO_2 concentration in the inhaled air was not maintained, in all simulated cases, below 1000 ppm (Fig. 6), while in the same simulated cases with DV the CO_2 concentration in the inhaled air did not exceed 770 ppm (Fig. 5). The quality of inhaled air was expected to be better with DV due to the air distribution principle. With DV, the air was distributed based on air density differences. In this way, the CO_2 contained in the exhaled air was lifted upwards by the free convection flow developed around the occupants, as well as due to the buoyancy of the exhaled air, resulting in a lower clean zone (breathing zone) and an upper polluted zone. On the other hand, with MV the clean outdoor air was supplied in such a way in order to be mixed with the indoor polluted air and achieve uniform CO_2 concentration equal to 1000 ppm. The personal exposure index, calculated by Eq. 4 [13], was between 0.94 and

1.02 for MV and within 1.58 and 2.88 for DV. Comparison of the current findings with those of other studies confirms that DV could provide better inhaled air quality than MV [13].

$$\varepsilon_{exp}^{c} = (c_e - c_s) / (c_{exp} - c_s) \quad (4)$$

Where, c_e is the CO_2 concentration in the exhausted air in ppm; c_s is the CO_2 concentration in the supplied air, 400 ppm; c_{exp} is the inhaled CO_2 concentration in ppm; ε_{exp}^{c} is the personal exposure index.

It can be seen in Fig. 5 and Fig. 6 that in all simulated cases, either with MV or DV, the concentrations monitored above the heads of occupants exhaling were much higher compared to the corresponding concentrations measured at the mouth of the exposed occupant. These findings were expected as the horizontal exhaled jet, containing 52778 ppm of CO_2, interacted with the convective boundary layer developed around the exhaling person, thus reducing the momentum of the exhalation flow. Then, the exhaled jet with reduced speed, still, penetrated the boundary layer of the exhaling occupant and interacted with the room airflow. Due to this interaction, the exhaled jet speed further decreased causing the jet to spread closer to the face of the exhaling occupant and raise upward. As a result, high concentrations were monitored above the heads of occupants exhaling.

3.1 Influence of the solar gains on exposure

In the reference case with DV, Occupant No. 6 was inhaling 603 ppm of CO_2 (Fig. 5). When solar gain of 200 W was simulated by attaching higher temperature to the surface of the window, compared to the temperature attached to the other surfaces, the exposure increased by 26.9 % (162 ppm, see Fig. 5). In the reference case with MV, the CO_2 concentration in the inhaled air of Occupant No. 6 was 1018 ppm (Fig. 6), while simulating the solar gain the exposure decreased by 4.6 % (46 ppm, see Fig. 6). Either with MV or DV, the CO_2 concentrations monitored above the heads of most of the occupants exhaling were considerably reduced when the solar gain was considered (Fig. 5 and Fig. 6).

In Case 2 with MV (Table 1), the upward convective flow produced in the vicinity of the window, due to the simulation of the solar gain, interacted with the downward flow of the cold and clean air supplied from the two ceiling diffusers. In Fig. 7 it can be seen that the air jets of the supplied outdoor air were “pushed away” in an opposite direction by the buoyancy flow generated by the window towards the location of Occupants No. 3 and No. 6. On the other hand, in the reference case (no solar gain) the direction of the air jets was towards the window (Fig. 7). Thus, in Case 2 the room air distribution resulted in higher air speed close to Occupants No. 3 and No. 6 and as a result better mixing of the clean supplied air with the polluted room air was achieved close to Occupant No. 6 compared to the corresponding reference case, in which no solar gains were simulated (Fig. 8). Kosonen et al. [21] documented similar results when they studied the influence of the heat load distribution on the air distribution in a test room. They found that the concentrated heat load on the right side of the room had as a result the development of strong thermal plume that pushed the air supplied from the chilled beams towards the left side of the room. Because of this airflow interaction, the air velocities on the left side of the room were higher than on the right side of the room.

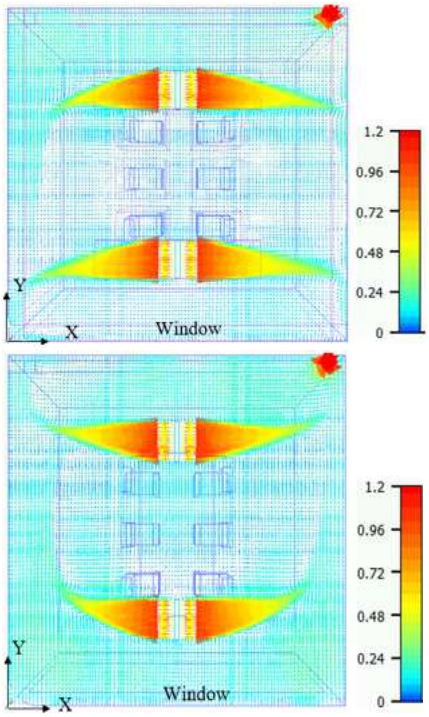

Fig. 7. Vectors of air speed (m/s) at the ceiling in Case 1 – no solar gain (top), and in Case 2 - solar gain of 200 W (down); MV, distance between the occupants facing each other of 1.4 m

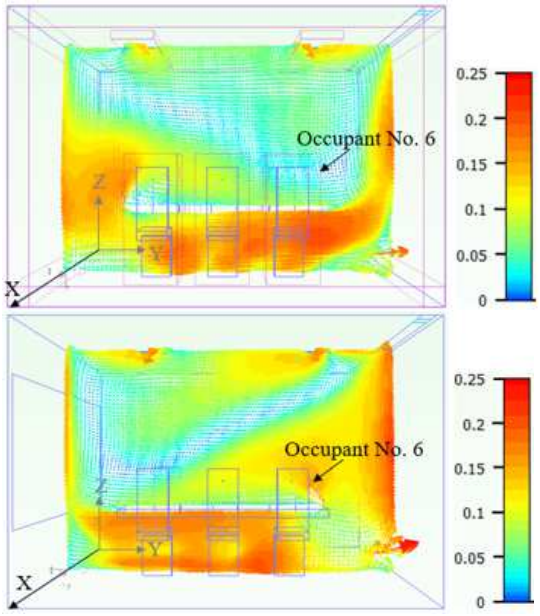

Fig. 8. Vectors of air speed (m/s) in the middle of the distance between the occupants facing each other (at x= 2.1 m) in Case 1 - no solar gain (top) and in Case 2 - solar gain of 200 W (down); MV, distance between the occupants facing each other of 1.4 m

In Case 2 with DV (Table 1), the upward convective flow produced by the window (located at 0.75 m above floor) created a warm horizontal air layer starting from 0.85 m height above floor and extending until above the heads of the occupants (see Fig. 9). In the reference case with DV (Case 1, Table 1), a warm horizontal air layer was created as well, but in this case, it started at 1.2 m above floor, mouth height (see Fig. 9). In Case 2, the warm horizontal air layer, which covered the whole upper body of the occupants, decreased the velocities of the upward free convection flow developed around the occupants. This in turn caused weaker upward transportation of the exhaled CO_2 and thus created a horizontal air layer with higher CO_2 concentration at the breathing zone, compared to the reference case. This effect, i.e. higher fraction of metabolic CO_2 stratified at the breathing zone height, explains also the lower concentrations above the heads compared to the reference case.

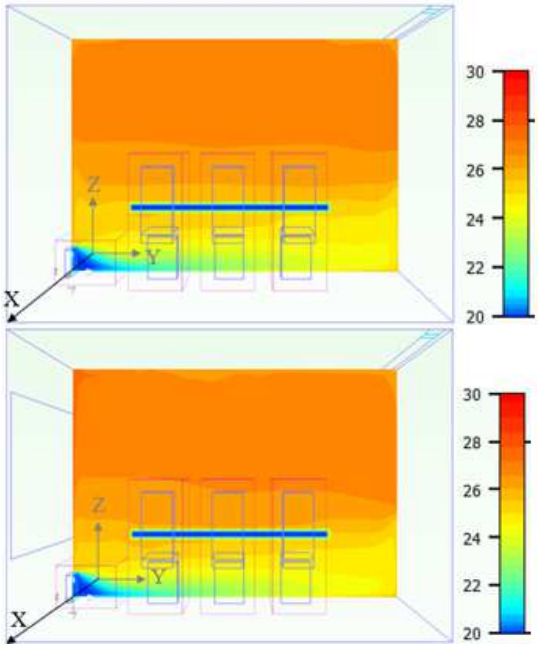

Fig. 9. Contours of temperature (°C) in the middle of the distance between the occupants facing each other (at x= 2.1 m) in Case 1 - no solar gain (top) and in Case 2 - solar gain of 200 W (down); DV, distance between the occupants facing each other of 1.4 m

3.2 Influence of the distance between the occupants facing each other on exposure

In the case of DV, when the distance between the occupants facing each other decreased from 1.4 m to 1.0 m (Case 3, Table 1) the CO_2 level in the inhaled air increased by 2.7 % (16 ppm, see Fig. 5), while the CO_2 concentrations monitored above the heads of most of the exhaling occupants decreased (see Fig. 5). These results might be due to the slightly higher vertical temperature gradient (only by 0.1°C/m) in the breathing zone when there was 1.0 m distance compared to 1.4 m distance. Bjørn and Nielsen [10] conducted a series of experiments in a DV chamber and they found that the exhalation flow through the mouth of both seated and standing person could stratify in the breathing zone height when the vertical temperature gradient in the breathing zone height exceeded 0.5°C/m. As a result, higher concentration could be observed locally. In the present CFD simulations, the vertical temperature gradient in the breathing zone height was higher than 0.5°C/m in both simulated cases (Case 1 and Case 3, Table 1). However, in the reference case with DV (distance between the occupants of 1.4 m, Case 1) the local vertical temperature gradient was approximately 0.9°C/m (measured in the breathing zone height), while when the distance decreased to 1.0 m (Case 3) the corresponding vertical temperature gradient was 1.0°C/m. Therefore, the exhaled flow in the case of small distance between the occupants facing each other stratified more than in the case with larger distance. As a result, in the case with 1.0 m distance larger fraction of CO_2 was spread out in the room horizontally, while in the case with 1.4 m distance larger fraction of CO_2 was transported upward (Fig. 10).

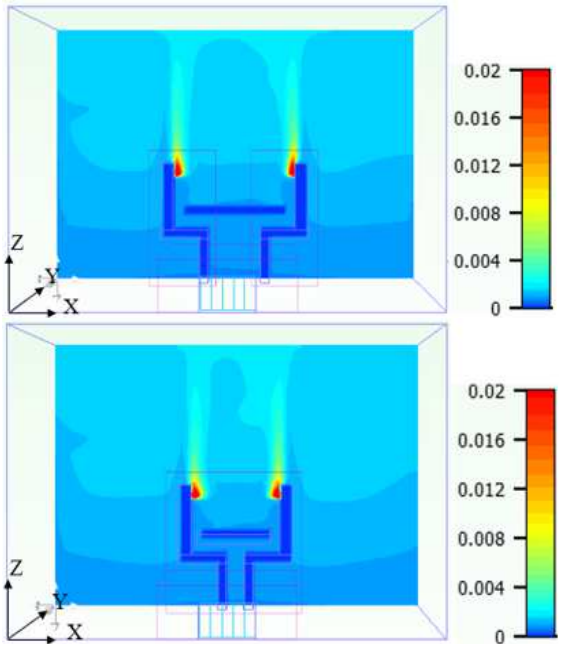

Fig. 10. Contours of CO_2 concentration (kg/kg) at the cross section of Occupants No. 1 and No. 4 (at y= 1.2 m) when the distance between the occupants facing each other was 1.4 m (top) and 1.0 m (bottom); DV, no solar gain

In Case 3 with MV (Table 1), when the distance between the occupants facing each other decreased from 1.4 m to 1.0 m, the CO_2 level in the inhaled air decreased by 1.3 % (13 ppm, see Fig. 6), while the CO_2 concentrations monitored above the heads of most of the exhaling occupants were reduced at least by 87 ppm (see Fig. 6). In mixing ventilated rooms, the CO_2 concentration at a location depends on the mixing level of the supplied clean air with the indoor polluted air. In Case 3, due to the shorter distance between the seated occupants, their convective boundary layers interacted with each other causing higher air speed in front of the breathing zone of the occupants and above the heads compared to the case with 1.4 m distance. This airflow

interaction is shown in Fig. 11. Therefore, in Case 3 the interaction of the convective boundary layers of the occupants promoted better mixing of room air, compared to the reference case, explaining the decrease in CO_2 concentrations monitored both in the inhaled air and above the occupants.

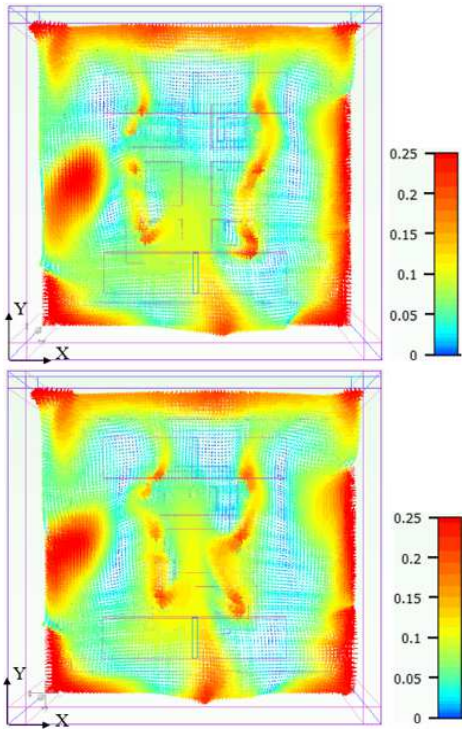

Fig. 11. Vectors of air speed (m/s) when the distance between the occupants facing other was 1.4 m (top) and 1.0 m (down), at 1.45 m above floor (10 cm above the heads)

4 Limitations

The breathing mode was simulated as constant flow rate. Although, the defined exhalation flow rate corresponded to the same pulmonary ventilation rate of an adult person performing sedentary activity [20], simulating the exhalation as constant flow could not capture its actual interaction with the room airflow. Villafruela et al. [22] found that using simplified steady conditions could not accurately predict the distribution of contaminants contained in the exhaled air.

The occupants were simulated to be seated by using three cuboids. Although the total surface area was realistic, 1.66 m^2, the shape was rather simple. Furthermore, the chairs were not simulated. That implies that the free convection flow developed around the occupants could differentiate from the actual one, and as a result the interaction of the room airflows could be different from the actual one. Especially, in the case of DV that the buoyancy forces of the room are used to transfer the pollutants from the occupied zone towards the upper room zone, the unrealistic modelling of the occupants' body might have affected the obtained results.

The radiant part of heat exchange was simulated by attaching the required temperature to the surfaces of envelope in order to obtain heat balance without enabling the radiation model in the CFD simulations.

5 Conclusion

This study investigated the influence of the heat gain from vertical surface (e.g. warm window due to solar gain) and the distance between the occupants facing each other on CO_2 concentration in the inhaled air under mixing air distribution and displacement air distribution. It was found out that the interaction of the buoyancy flow generated by the heated vertical surface with the other flows in the room can increase the exposure to metabolic CO_2 by 26.9 % in a room with displacement ventilation and reduce the inhaled CO_2 by 4.5 % in the case of mixing ventilated room. The distance between the occupants could not be considered as an important factor influencing the exposure, as decreasing the distance by 0.4 m (from 1.4 m to 1.0 m), the exposure increased by 2.7 % in the case of DV, while it decreased by 1.3 % in the case of MV.

References

1. P. Wargocki, *Ventilation, Indoor Air Quality, Health, and Productivity*. [forfatter] A. Hedge, *Ergonomic Workplace Design for Health, Wellness, and Productivity* (2016)
2. B. Heinzow & W. Butte, Rev. Environ. Contam. Toxicol. **175**, 1-46 (2002)
3. N.Y. Hsu, C.C. Lee, J.Y. Wang, Y.C. Li, H.W. Chang, C.Y. Chen, C.G. Bornehag, P.C. Wu, J. Sundell and H.J. Su, Indoor Air, **22**(3), 186-199 (2012)
4. Executive order on building regulations 2018 (BR18)
5. S.J. McBride, A.R. Ferro, W.R. Ott, P. Switzer, L.M. Hildemann, Journal Exposure Analysis and Environmental Epidemiology, **9**(6), 602-21 (1999)
6. D. Rim & A. Novoselac, Building and Environment, **44**(9), 1840-1849 (2009)
7. D. Rim & A. Novoselac, Journal of Occupational and Environmental Hygiene, **7**(12), 683–692 (2010)
8. M.P. Bivolarova, J. Ondráek, V. Ždímal, A.K. Melikov, Z.D. Bolashikov, *Exposure to aerosol and gaseous pollutants in a room ventilated with mixing air distribution,* In Proceedings of Indoor air (2016)
9. A.K. Melikov & J. Kaczmarczyk, Indoor Air, **17**(1), 50-9 (2007)
10. E. Bjørn & P.V. Nielsen, Indoor Air, **12**(3), 147-64 (2002)
11. D. Müller, C. Kandzia, R. Kosonen, A.K. Melikov, P.V. Nielsen, *Revha Guidebook No.19, Mixing ventilation - Guide on mixing air distribution design* (2013)
12. D. Licina, A.K. Melikov, C. Sekhar, K.W. Tham, Science and Technology for the Built Environment, **21**(8), 1175-1186 (2015)

13. R. Kosonen, A.K. Melikov, E. Mundt, P. Mustakallio, P.V. Nielsen, *Revha Guidebook No.23, Displacement ventilation* (2017)
14. H. Awbi, *Ventilation of buildings* (2003)
15. DS/ EN 15251, *Indoor environmental input parameters for design and assessment of energy performance of buildings addressing indoor air quality,* thermal *environment, lighting and acoustics* (2007)
16. D. Zukowska, A.K. Melikov, Z. Popiolek, Building and Environment, **49**, 104-16 (2012)
17. N. Gao & J. Niu, Building and Environment, **41**(9), 1214-1222 (2006)
18. J.K. Gupta, C.H. Lin, Q. Chen, Indoor Air, **20**(1), 31-39 (2010)
19. T. Zhang, S. Yin, S. Wang, Building and Environment, **46**(10), 1928-1936 (2011)
20. C.E. Hyldgård, *Humans as a source of heat and air pollution,* Proceedings of Roomvent 1994, pp. 413-433, 4th International Conference on Air Distribution in Rooms, Krakow Poland (1994)
21. R. Kosonen, A.K. Melikov, B. Yordonova, L. Bozkhov, *Impact of heat load distribution and strength on airflow pattern in rooms with exposed chilled beams,* Proceedings of Roomvent 2007a, 10th International Conference on Air Distribution in Rooms, Helsinki (2007)
22. J.M. Villafruela, I. Olmedo, M. Ruiz de Adana, C. Mendez, P.V. Nielsen, Building and Environment, **62**, 191-200 (2013)